The Creation of a Brain Atlas for Image Guided Neurosurgery using Serial Histological Data

M. Mallar Chakravarty[1], Gilles Bertrand[1,3], Maxime Descouteaux[2], Abbas F. Sadikot[1,3], and D. Louis Collins[1].

[1] Montreal Neurological Institute (MNI), McGill University, Montreal Canada
[2] Center for Intelligent Machines (CIM), McGill University, Montreal Canada
[3] Division of Neurosurgery, McGill University, Montreal Canada

Abstract. Digital atlases of the human brain can help in the specific localization of structures of surgical relevance and interest in Image Guided Neurosurgery (IGNS). This paper outlines one of the steps in the creation of a digital atlas intended for IGNS, using histological data. The acquisition of histological data can include artefacts such as tearing, shearing, stretching, shrinking, as well as inhomogeneous staining leading to structural inhomogeneities. These inconsistencies are reduced using a non-linear intensity based registration procedure where deformations are defined using a maximized correlation coefficient estimate. The intensity artefacts brought about by inhomogeneous staining are reduced by applying a slice to slice intensity inhomogeneity correction by modelling the intensity mapping between slices as a third order polynomial that is estimated with a Least Trimmed Squared fit. The final step is to subsample this data to achieve near isotropic sampling and to improve the appearance of the data. To demonstrate improvements, the lateral ventricle was then segmented and the principle curvatures of the zeroth order level set were calculated at each point on its surface. Using the standard deviations of the mean and Gaussian curvatures, we show a decrease in the roughness of the surface, indicating improved structural alignment with our method.

1 Introduction

Though several anatomical imaging methods exist, these methods are not always adequate in planning neurosurgical procedures. Imaging modalities such as Magnetic Resonance Imaging (MRI), Positron Emission Tomography (PET), and Computed Tomography (CT) do not allow for a detailed analysis of certain structures in the brain due to their spatial resolution limitations. Digital or computerized atlases can help improve the accuracy and precision of the spatial localization of a region of interest within a patient's brain when used in conjunction with different imaging modalities [1, 11].

The goal of Image Guided Neurosurgery (IGNS) is to use data from different imaging modalities in order to help plan stereotaxic neurosurgical procedures. Using this data, surgeons are able to interpret patient specific image volumes

of anatomical, functional, and vascular relevance as well as their relationships. However, atlases can provide histological, functional or cyto-architectonic information to enhance a surgeon's visualization and understanding[1, 11]. Atlases of the basal ganglia and thalamus are required to determine stereotaxic targets for surgical treatment of movement disorders, such as tremor associated with Parkinson's disease [1]. In the standard stereotaxic method, linear scaling is used to fit an atlas to a patient's anatomy [12]. Our group was among the first to use a non-linear registration to improve atlas warping, thus enhancing positional targeting in patient's anatomy [11].

The creation of an atlas from histological data is a three-dimensional (3-D) problem and slices of histological data are two-dimensional (2-D). In most cases, anatomical structures are defined by an anatomist on the 2-D slices. This 2-D data must be reconstructed (tessellated) to create a 3-D geometric atlas that can be mapped to any patient's anatomy. Unfortunately, the acquisition of histological data contains artefacts such as tearing, shearing, stretching, shrinking or other types of morphological inconsistencies. If the 2-D data is reconstructed into 3-D by simply stacking the 2-D histological data, these morphological inconsistencies will be present in the reconstruction. This includes non-homogeneous structural definitions in addition to poorly defined and unsmooth surfaces. Inconsistent lighting and staining can also cause intensity inhomogeneities in reconstructions of the stacked histological data. In this paper we present initial work to correct the histological data by improving slice-to-slice alignment while correcting for some intensity artefacts.

Other work has been done in creating digital atlases using histological data. Ourselin *et al.*[8] used an intensity based block-matching strategy between slices of histological data and a Least-Trimmed Squared (LTS) minimization in order to define rigid or affine transformations from the source block to the target block. A 3-D registration from the reconstructed volume with a reference MRI was done using a similar block matching strategy. Toga *et al.*[13] used a fiducial marker based registration process to align serial sections. Their method uses a combination of local and differential scaling to put anatomical data in Talairach space [12]. Kim *et al.*[7] used a thin-plate spline (TPS)[2] technique to reconstruct a set of rat brain autoradiographs to a video block face reference. The TPS is a landmark based registration where the deformation between analogous landmarks is calculated using *n-th* order polynomials. Kim*et al.* implemented their technique using landmarks defined on a grid or circle, that did not necessarily have any anatomical significance.

We propose a new technique in the creation of a digital atlas using histological data for which no complementary data (such as complementary MRI data or digital photographs of the blockface) is available. There are several cryogenic and histological datasets in existence which are of high quality, have been studied extensively, and pre-date the use of brain-imaging modalities or digital photography. The goal of our research is to create a 3-D reconstructed volume of such data while minimizing morphological variability introduced in the data acquisi-

tion process. Section 2 will describes the acquisition of the data while Section 3 describes the 3-D reconstruction technique.

2 Histological Data Acquisition

The histological data set used here was acquired in 1957 from a male patient who died of non-neurological complications. The brain was removed and fixed in 10% formalin and suspended in a gauze hammock to avoid any deformation. The brain was then split at the midline after which a block, centered on the thalamus and measuring 6cm from front to back, 4.4cm from top to bottom, and 3.2cm from side to side, was sectioned out. The volume contains all of the basal ganglia together with the amygdala and the hippocampus (except for the posterior portion).

After dehydration the block was mounted in paraffin and placed in a microtome. Slices were taken at 0.69mm intervals between sections. Alternating sections were stained with Luxol Blue for myelin and with a Nissl stain for cell bodies. Corresponding myelin and cell photographs were then placed together and matched on the histological data as closely as possible. The contours structure were then segmented by hand by a neuroanatomical expert (GB) using Adobe Photoshop.

3 3-D Reconstruction Methods

The 3-D reconstruction used a three step approach. Prior to implementing the reconstruction scheme the contours and the histological images were seperated. A picture of all three of these images can be seen in Figure 1. The colour photographs of the stained image were then converted to grey-level images. These images are considered in the reconstruction scheme described.

First a registration scheme was implemented in order to align homologous anatomical structures between sections. An intensity inhomogeneity correction was then implemented to correct any lighting artefacts and inconsistent staining which may have occurred in the original data acquisition. The volume was then super-sampled to obtain near-isotropic resolution. These steps are described in the following sections.

3.1 Registration

The Automatic Nonlinear Matching and Anatomical Labeling(ANIMAL) registration scheme was used to reduce the morphometric variability between slices [4, 5]. The registration scheme is based on a 2-D lattice defined for each slice which makes up the volume. A deformation vector is then calculated for each node on the lattice. Each deformation vector is estimated by maximizing the correlation coefficient of the local intensity neighborhood centered at each lattice point. Since we have no reference data we maximize anatomical consistency between slices.

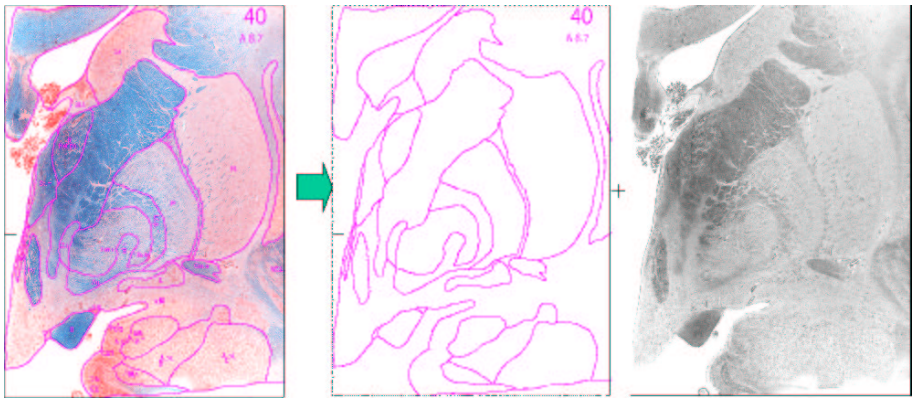

Fig. 1. An example of the data set. Left: The colour data with segmentation lines drawn. **Middle:** The segmentation contours. **Right:** Grey-level image.

In doing the non-linear registration we consider the data sequentially in sets of three slices. Let the source be the second slice in the sequence of three slices. Let the two extreme slices in this set be the targets. All three slices in the set were blurred with an isotropic Gaussian kernel. Two different deformation vector fields were calculated to define the warp from the source slice to each of the target slices. The average of these two deformation vector fields was then applied to the source slice, thus maximizing its similarity with both targets simutaneously. We then incremented our procedure by a slice and consider the next set of three slice (the source slice from the previous step is now a target slice, and one of the target slices from the previous step is now a source slice).

The voxel size of each slice was 34μm x 34μm x 700μm. Based on this resolution, the blurring was done with a Gaussian kernel with a Full Width at Half Maximum (FWHM) of 640μm. The deformations were calculated over 50 iterations using a step size of 1700μm and a lattice diameter of 3400μm.

It should be noted here that this registration procedure will not account for any global deformations. For example, uniform shrinkage throughout the data set cannot be accounted for since there is no reference. Local anatomical inconsistencies between slices are accounted for by this process.

3.2 Intensity Inhomogeneity Correction

Intensity artefacts are also incurred during the acquisition of the histological data. Inhomogeneous lighting and inconsistent staining can cause artefacts in the intensity of the 3-D reconstructed volume. The intensity inhomogeneity correction scheme developed by Prima *et al.*[9] was used. The technique models the intensity mapping of one image to another as a polynomial with degree greater than order one. This mapping is then applied to all the pixels in the image. We applied a third order polynomial for each image after which an LTS fit was applied.

Here we considered the data sequentially in groups of two slices. Let the second slice in this set be the target image. Let the first slice in this set be the reference image. The LTS fit is calculated between the target and reference images. The correction is then applied to the target image. We then increment the procedure by a slice and consider the next set of two slices (the target image from the previous step is now the reference image). We consider the spatial variation between slices in the histological data set to be small enough to be accommodated by the technique.

3.3 Super-sampling

After all the intensity corrections and registration corrections have been applied, the volume is then super-sampled along the z axis, creating additional smoothing. The sampling was increased by a factor of ten, using trilinear sampling. This creates a final voxel size of 34μm x 34μm x 70μm.

4 Results

Figure 2 shows a pictoral view of the results. The first three pairs of images are the pre-registration step and post-registration step images. The box represents the region of interest shown in Figures 3 after super-sampling of the intensity inhomogeneity has been applied to the un-registered and registered data.

Figure 2 shows the uncorrected and corrected data. Streaking caused by intensity inhomogeneities has decreased in the corrected data. Figures 3 show both data sets after the inhomogeneity correction has been applied and the data has been super-sampled. The close-up on the right shows that the contour has been smoothed.

To quantify the smoothness of the end result, the lateral ventricle was manually segmented at each slice in the volume. A surface rendering of this segmentation was done and the curvature of this surface was also analyzed. Figure 4 below shows a view of the reconstructed ventricles of both the spatially corrected and uncorrected volumes. These surfaces can be seen in Figure 4. Although the differences between the surfaces are subtle, our analysis of the principle curvatures demonstrate greater smoothness quantitatively.

Mathematically, any surface can be characterized by its two principle curvatures, which are two orthogonal vectors. The principle curvatures roughly represent the shape (including any perturbations) of a surface. The mean curvature is simply the average of the two principle curvatures and the Gaussian curvature is their product [6]. A decrease in curvature indicates that a surface is smoother.

The level set approach is used for calculating the mean curvature and the Gaussian curvature for every voxel on the surface rendering of the ventricle [3]. This is done in a two step process. First the distance transform for the binary volume is calculated in order to obtain the zeroth order level set. This corresponds to the 3-D outside surface of the segmented ventricle. The second step involves the calculation of the mean and Gaussian curvatures based on the

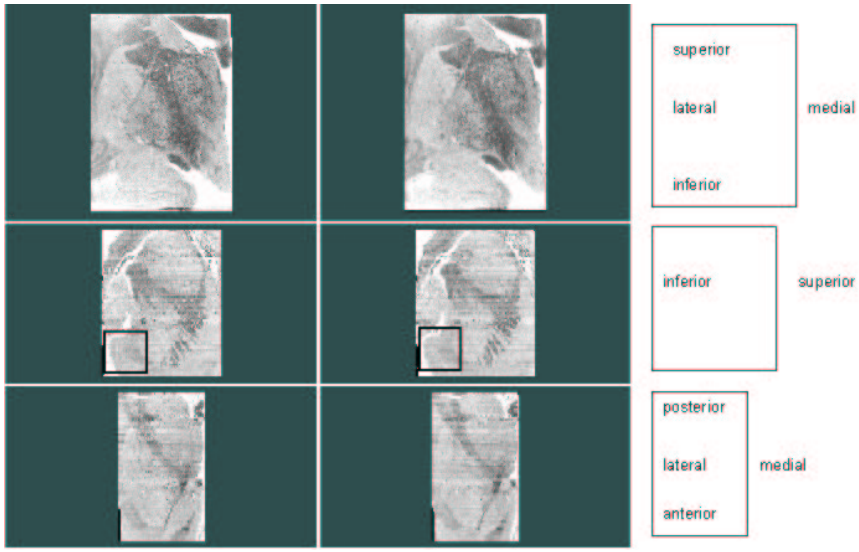

Fig. 2. Volumes before and after registration correction Left: The original, uncorrected data. **Middle:** The post-registration and intensity inhomogeneity-corrected output. **Right:** Orientation. **Top:** Coronal View. **Middle:** Saggital View. **Bottom:** Transverse View. The boxed region will be the focus of Figures 3.

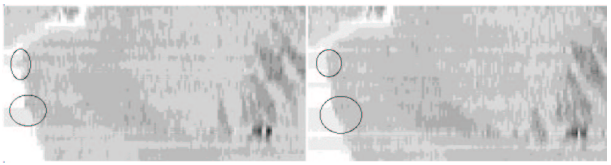

Fig. 3. Close-up of volumes before and after registration correction. Left: The data after performing intensity inhomogeneity correction and supersampling but not the registration correction. **Right:** Corrected data. Smoothing of the edge has occurred.

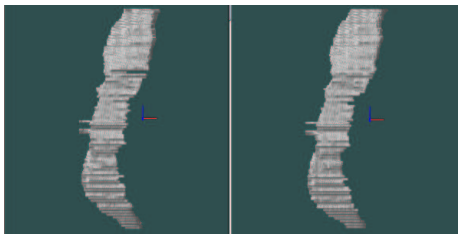

Fig. 4. Top view of the Lateral Ventricle. Left: Segmented lateral ventricle before registration correction. **Right:** Segmented lateral ventricle after registration correction.

distance transform function[10]. The average and standard deviations for both these curvatures, are shown in Table 1.

Table 1. Average and Standard Deviation for the Mean and Gaussian Curvatures Values for each Voxel on 3-D Lateral Ventricle Surface.

	Mean Curvature	Standard Deviation
Before Correction	2 081.7	15.5
After Correction	1 646.6	10.74

	Gaussian Curvature	Standard Deviation
Before Correction	16 879	254.26
After Correction	9 641	125.11

We can see from Table 1 that the mean curvature has decreased by 21% and that the Gaussian curvature has decreased by 42%, indicating that the surface of the reconstructed ventricle is much smoother due to the alignment technique described here.

5 Conclusion

This atlas is intended for use with an IGNS system and when complete, it would replace the simple stereotaxic atlas in use [11]. This would be the first step towards a full integration of this atlas in an IGNS platform.

This work is also done with older data which has no block-face or MRI reference. This method should be tested against results obtained with reference data to see how it compares with such methods.

An intensity inhomogeneity scheme better suited to histological data is also necessary. Although the correction scheme used here yields global slice-to-slice intensity correction, it is not optimized for spatially variant inhomogeneity between slices. An adaptive thresholding technique, is being considered. This technique would examine a neighborhood of pixels and use a polynomial fit between a reference slice and the target slice.

We have presented here a method to reconstruct histological data, while accounting for anatomical inconsistencies and slice to slice intensity inhomogeneities. The results demonstrate increased smoothness of the reconstructed volume. This will allow us to proceed in creating a 3-D geometric atlas of the basal ganglia and thalamus for use in stereotaxic IGNS.

References

[1] J. Atkinson, D.L. Collins, G. Bertrand, T.M. Peters, B. Pike, and A.F. Sadikot. Optimal location of thalamotomy lesions for tremor associated with Parkinson disease: a probablisitic analysis based on postoperative magnetic resonance imaging and integrated digital atlas. *Journal of Neurosurgery*, 96(5):672–680, October 2002.

[2] F.L. Bookstein. Principal Warps: Thin-Plate Splines and the Decompostion of Deformations. *IEEE Transactions on Pattern Analysis and Machine Intelligence*, 11(6):567–585, 1989.

[3] G. Borgefors. Distance Transformations in Arbitrary Dimensions. *Computer Vision, Graphics, and Image Processing*, 27:321–345, 1984.

[4] D.L. Collins, P. Neelin, T.M. Peters, and A.C. Evans. Automatic 3D Intersubject Registration of MR Volumetric Data in Standardized Talairach Space. *J. of Computer Assisted Tomography*, 18(2):192–205, March 1994.

[5] L. Collins, T.M. Peters, and A.C. Evans. An Automated 3D non-linear image deformation procedure for Determination of Gross Morphometric Variability in Human Brain. In Richard A. Robb, editor, *VBC*, volume 2359 of *SPIE*, Rochester (Minnesota) (USA), 1994.

[6] H.W. Guggenheimer. *Differential Geometry.* Mc-Graw-Hill Book Company, New York, USA, 1963.

[7] B. Kim, J.L. Boes, K.A. Frey, and C.R. Meyer. Mutual Information for Automated Unwarping of Rat Brain Autoradiographs. *Neuroimage*, 5:31–41, 1997.

[8] S. Ourselin, E. Bardinet, D. Dormont, G. Malandain, A. Roche, N. Ayache, D. Tandé, K. Parain, and J. Yelnik. Fusion of histological sections and mr images: Towards the construction of an atlas of the human basal ganglia. In *Medical Image Computing and Computer-Assisted Intervention (MICCAI)*, pages 743–751, Utrecht, Netherlands, October 2001.

[9] S. Prima, N. Ayache, Tom Barrick, and Neil Roberts. Maximum Likelihood Estimation of the Bias Field in MR Brain Images: Investigating Different Modelings of the Imaging Process. In Wiro J. Niessen and Max A. Viergever, editors, *Fourth International Conference on Medical Image Computing and Computer-Assisted Intervention, MICCAI'2001*, volume 2208 of *Lecture Notes in Computer Science*, pages 811–819, Utrecht, Netherlands, October 2001. Springer.

[10] J.A. Sethian. *Level Set Methods.* Cambridge University Press, 1996.

[11] P. St-Jean, A.F. Sadikot, L. Collins, D. Clonda, R. Kasrai, and A.C. Evans. Automated Atlas Integration and Interactive Three-Dimensional Visualization Tools for Planning and Guidance in Functional Neurosurgery. *IEEE Transactions on Medical Imaging (TMI)*, 17:854–866, May 1998.

[12] J. Talairach and P. Tourneau. *Co-Planar Stereotaxic Atlas of the Human Brain.* Georg Thieme Verlag, Stuttgart, Germany, 1988.

[13] A.W. Toga, A. Goldkorn, K. Ambach, K. Chao, B.C. Quinn, and Y. Yao. Postmortem Cryosectioning as an Anatomic Reference for Human Brain Mapping. *Computerized Medical Imaging and Graphics*, 21(2):131–141, 1997.